An Analysis of Neutron Yield by Spallation using various Target Materials

Outreach Proposal

The Quantum Neutronauts

Aadi Kothari, Aarav Jalan, Aarav Shah, Annan Vora, Dhruv Chopra, Keshav Mohta, Kiara Maniar, Param Davda, Raahil Mullick, Rishi Mody, Ritisha Bansal.

Dhirubhai Ambani International School, Mumbai, India.

April 2024

Contents

1 Our Motivation

Participating in the CERN BL4S competition offers us an exceptional chance to delve into the forefront of modern particle physics. While classroom learning covers laboratory experimentation and theoretical concepts, this competition empowers us to go beyond the bounds of our school education and leverage state-of-the-art physics technology. United by our passion for the subject, the opportunity to represent India and conduct experiments at renowned facilities like T9 or DESY motivates us to put forth our best efforts.

2 Introduction and Background Information

2.1 Spallation Neutron Source

Traditionally, neutrons were produced by the spontaneous fission of different sources in fission reactors.[1] However, an alternate method with many advantages was found: a nuclear reaction known as spallation that leads to an almost complete disintegration of nuclei. This reaction involves bombarding a target with high-energy protons from an accelerator, releasing a large number of neutrons alongside protons, mesons, nuclear fragments, and γ radiation.

The Spallation reaction occurs in two stages. In Stage 1, high-energy protons collide with atomic nuclei, causing nucleons to be ejected in a cascading reaction within the nucleus. The ejected nucleons may further collide within the same nucleus or with nucleons in neighbouring nuclei. In Stage 2, the excited nuclei release their stored energy through evaporation, emitting particles such as neutrons, protons, and fragments, along with gamma radiation. Among these, the emitted neutrons are particularly significant and exhibit a spectrum similar to that of nuclear fission. Figure 1 below showcases the same.

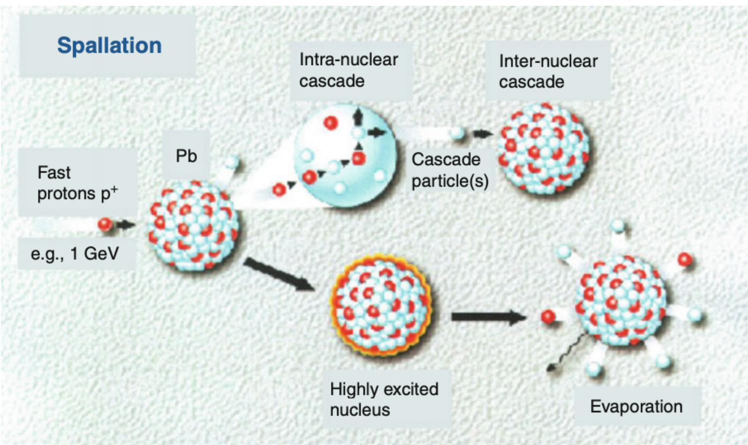

Figure 1: A Graphic Representation of Spallation[2]

2.1.1 The Beam

The spallation reaction demands protons with energies greater than 100 MeV. The Proton Synchrotron (PS) at CERN has a primary beam composed purely of protons with energies up to 26 GeV, while its secondary beams has particles with energies between 0.2 and 15 GeV.[3] It is therefore the optimal beam to conduct this experiment.

2.1.2 Targets

The targets used for spallation are usually elements with high atomic numbers (e.g. tungsten, lead, and mercury) due to their high number of neutrons. Through this experiment, the neutron yield of different materials will be checked – namely for mercury, tungsten and lead. An approximate empirical expression for this has been found and can be checked through this experiment.

$Y = 0.1 \times (A + 20) \times (E - E_0)$[5]

- Y : Yield (Neutrons per Proton)
- A : Mass Number of Target Material
- E : Proton Energy
- E_0 : 0.12 GeV

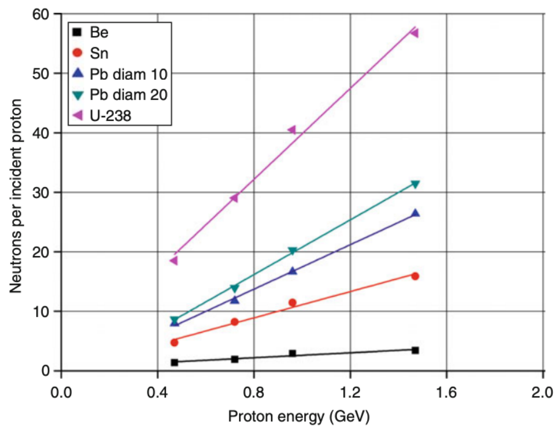

Figure 2: Neutron Yield of Different Materials [4]

3 Aim of the Experiment

Our experiment aims to compare the neutron yield produced by different heavy metal targets through the spallation process. By examining the suitability of different materials for use as targets, we can analyse neutron behaviour and their interactions with various forms of matter. This research holds particular relevance across diverse fields such as biology, materials science, chemistry, particle physics, engineering, and medicine [6], all of which extensively utilise neutrons in their studies.

4 Experiment Design

4.1 Experimental Setup

We will use the PS beamline at CERN, starting with beam energy 0.5 GeV and taking readings in increments of 0.5 GeV of beam energy up to 5.0 GeV (i.e. 0.5, 1.0, 1.5, 2.0, ..., 5.0).

4.1.1 Neutron Production & Isolation

The experiment's first part is the production and isolation of neutrons from the other products of spallation.

- To eventually find the neutron yield per proton, the protons must be counted at the start. This can be done by using a collimator to concentrate the proton beam onto a DWC (Delay Wire Chamber). The DWC, or an array of them, can count protons without interfering with their motion[7].
- The protons continue to the spallation target. Lead, mercury, and tungsten will be the three tested targets; each will be tested in different instances of the experiment. As mentioned earlier, the spallation reaction would produce protons, neutrons, gamma rays, and nuclear fragments.
- Protons and nuclear fragments are now separated using a dipole magnet. The dipole magnet would separate charged particles while allowing neutrons, which are neutral particles, to pass.
- The neutrons be directed to a detector for them using neutron guides: glass conduits coated with a special material optimized for neutron reflection – either nickel or chromium [8].

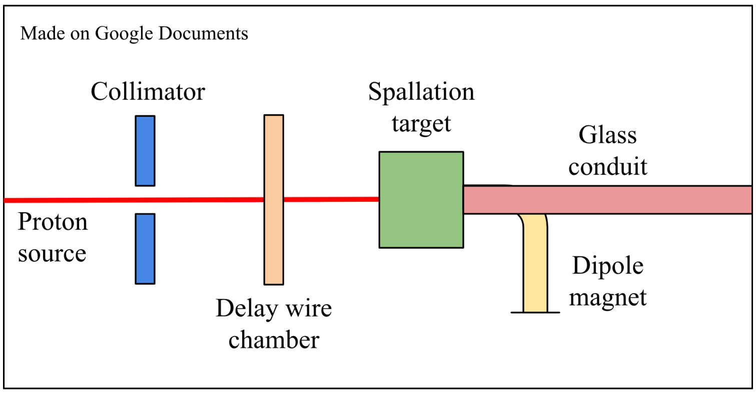

Figure 3: The first half of the experimental setup

4.1.2 Neutron Detection

Generally, due to neutrons being uncharged, they cannot be detected directly, which is why the secondary products of their reactions with different materials must be used to count or detect them. Two approaches can be taken, and these are: proportional counters and scintillation detectors.

Proportional Counters

Proportional counters use gases such as helium-3 or boron tri-fluoride. When these gases interact with neutrons, ionization occurs, and the resulting ion pairs are then collected and amplified. This experiment will use the BF_3-filled proportional counter as it is one of the most widely used neutron detectors. The following equation shows the reaction that takes place:

$$n + B_5^{10} \rightarrow Li_3^7 + \alpha + 2.79MeV$$

This produces an electrical signal that can be counted to determine the number of neutrons detected. [9] It must be taken into account that neutrons produced by spallation are too fast for proportional counters and hence must be slowed down by a material called a moderator. Water, graphite, and heavy water are some moderators that can be used.

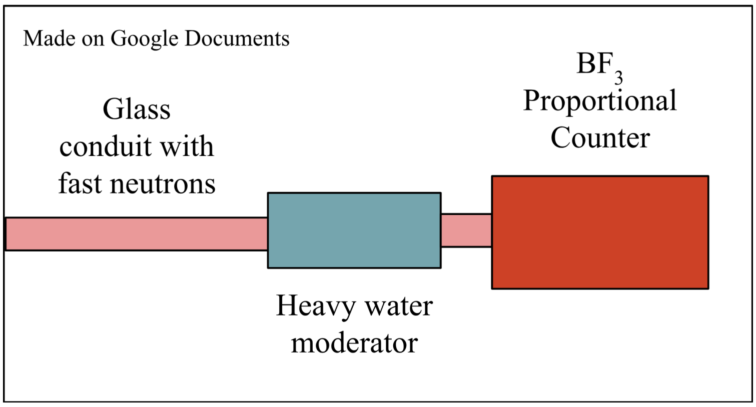

Figure 4: The setup for a BF_3 proportional counter

Scintillation Detectors

If proportional detectors are not available, scintillation neutron detectors are the next best alternative. These detectors consist of a scintillating material that emits light when struck by a neutron. The emitted light is then amplified using a photo-multiplier. The intensity of the light signal is proportional to the number of neutrons detected, allowing for neutron counting. While these detectors can effectively count neutrons, the materials they require may not be readily available, and hence, they may not be feasible to use.

4.2 Data Analysis

With the protons being counted by the DWC earlier, and the neutrons being counted by a proportional counter, we can calculate the experimental value for neutrons per incident proton:

$$Y = \frac{n}{p}$$

Where:

- Y = Neutron yield per incident proton.
- n = Number of neutrons counted.
- p = Number of protons counted.

Repeating this experiment for mercury, lead, and tungsten, and repeating the experiment at different proton energies for each of the targets will allow us to create a graph for Y against proton energy, like Figure 2. Plotting the graph for all targets on the same set of axes would allow us to find the highest-yielding target. We can also use the approximate empirical expression for neutron yield from section 2.1.2 to compare the expected literature values with our experimental values and thus see how accurate our readings are.

5 What We Hope to Take Away from the Experience

Through investigating spallation across diverse target materials, we not only aim to deepen our understanding of neutron production but also to enhance our practical skills, particularly in working with particle accelerators. This hands-on experience will allow us to refine our abilities in experimental physics, data analysis, and instrumentation, providing valuable insights into cutting-edge research technologies.

6 Outreach Activities Proposal

In Asia's largest slum, Dharavi, we want to transform one of the narrow gullies into a colourful STEM fair, where we will host a competition for children aged 8−12 in groups of 5.

The competition will comprise 3 tents or stages:

- **Tent 1: Rocket Science Workshop**
  Children will be given chart paper, tape, and scissors using which they have to build a model rocket. A fan will be used to blow air on the rocket and it must not fall over.
- **Tent 2: Magnetic Art**
  The children are given a range of magnets and iron filings. In each round, a different shape is shown on screen, and contestants must construct the shape's outline using magnets and filings.
- **Tent 3: Circuit Builders**
  Children will be given an Arduino breadboard. Challenges like building circuits for LEDs or parallel/series configurations will boost interest and scientific knowledge. **Note**: We will take all necessary safety precautions associated with the use of electricity.

To spread awareness, we designed an **outreach manual:**
https://drive.google.com/file/d/1XUiy5O83h8VjOgSSeaUWhYue2yoV7jHB/view.

The Top 3 teams will receive Physics tool-kits containing:

- **Breadboard Kit:** Including a battery and wires.
- **Toy Magnets**: Including a magnetic bracelet!
- **Infrared (Gun) Thermometer**

To further promote inclusivity and diversity, the competition will be conducted in different languages, including English, Hindi, and Marathi.

7 Acknowledgements

We would like to extend our heartfelt gratitude and appreciation to the following people and organisations:

- **Our School, DAIS:** For providing us with the resources required for scientific exploration and increasing our intellectual capabilities.

- **Our School Mentors:** Mr. Murali S and Dr. Chandana Ghosh for introducing us to this competition, and graciously guiding us through this process.
- **Our National Contacts:** Dr. Gunn Khatri for clarifying any technical, particle-physics-related doubts we had.
- **CERN BL4S's Team:** For continuously responding to our doubts, requests, and queries on emails (Sarah Maria Zoechling), and for hosting an incredible competition for high school students.

Thank you.

References

[1] Holmes, R. n.d. "GAMMA-RAY and NEUTRON SOURCES." https://inis.iaea.org/collection/NCLCollectionStore/_Public/14/792/14792880.pdf.

[2] Handbook of Particle Detection and Imaging / 1. 2012. Berlin ; Heidelberg: Springer.

[3] BL4S, CERN. 2024. "Beam and Detectors Beamline for Schools 2024." https://beamline-for-schools.web.cern.ch/sites/default/files/Beams_Detectors_BL4S2024.pdf.

[4] Syed Naeem Ahmed. 2017. Physics and Engineering of Radiation Detection.

[5] Carpenter, John M. 1977. "Pulsed Spallation Neutron Sources for Slow Neutron Scattering." Nuclear Instruments and Methods 145 (1): 91–113. https://doi.org/10.1016/0029-554x(77)90560-2.

[6] "What Can Be Studied with Neutrons? - Scientific Disciplines - Neutron Research - the NMI3 Information Portal." n.d. Nmi3.Eu. https://nmi3.eu/neutron-research/scientific-disciplines.html

[7] Spanggaard, J. 1998. "EUROPEAN ORGANIZATION for NUCLEAR RESEARCH European Laboratory for Particle Physics DELAY WIRE CHAMBERS a USERS GUIDE." https://cds.cern.ch/record/702443/files/sl-note-98-023.pdf.

[8] "Index." 2000. Nuclear Instruments and Methods in Physics Research Section A: Accelerators, Spectrometers, Detectors and Associated Equipment 452 (3): 533–42. https://doi.org/10.1016/s0168-9002(00)00945-1.

[9] L'annunziata, Michael F. 2020. Handbook of Radioactivity Analysis. Volume 1, Radiation Physics and Detectors. Amsterdam: Academic Press.

A Comparative Analysis of Photo Multiplier Tubes and Silicon Photo Multipliers in the Detection of Photons

The Quantum Detectors

Aadi Kothari, Aarav Jalan, Aarav Shah, Annan Vora,
Dhruv Chopra, Keshav Mohta, Kiara Maniar, Param Davda,
Raahil Mullick, Rishi Mody, Ritisha Bansal.

Dhirubhai Ambani International School, Mumbai, India.

April 2024

Contents

1 Our Motivation to Participate in BL4S

BL4S offers a unique opportunity for students to engage in hands-on research at the forefront of particle physics. We are excited at the prospect of using cutting-edge technology to achieve a potential breakthrough in the field. Tied together by our passion for the subject, the prospect of representing India and performing an experiment at CERN or DESY would be a dream come true for us.

2 Aim of the Experiment and Motivation

We aim to compare the performance of a Photo-Multiplier Tube (PMT) and a Silicon Photo-Multiplier (SiPM) to read out the photons emitted by a scintillator. The correct choice between these sensors could help improve the efficiency of scintillation counters, which are useful in radioactive surveys, biomedical imaging, nuclear plant safety, and cancer research.

PMTs are much costlier than SiPMs. As such, if SiPMs prove to be a decent alternative to PMTs from a scientific accuracy viewpoint, then that would be a success in finding an alternative to traditional PMTs.

3 Introduction and Background Information

3.1 Scintillation Counters

Each electron possesses a specific energy, referred to as its ‘electronic energy level’. When electrons absorb energy due to a particle passing through the material, they undergo excitation and transfer to an orbital with a higher electronic energy level. They then re-emit this absorbed energy in the form of photons.

Scintillators are materials that emit scintillator light, a property of luminescence, when excited by ionizing radiation.[1] This scintillator slab is connected to an electronic light sensor, which uses Einstein’s photoelectric effect to convert the photons into an amplified electrical pulse, which can be analysed to provide insights into the particle that struck the scintillator.

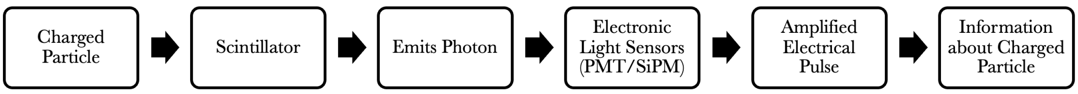

Figure 1: The Operation of a Scintillation Counter

3.2 Electronic Light Sensors

3.2.1 Photo Multiplier Tubes (PMTs)

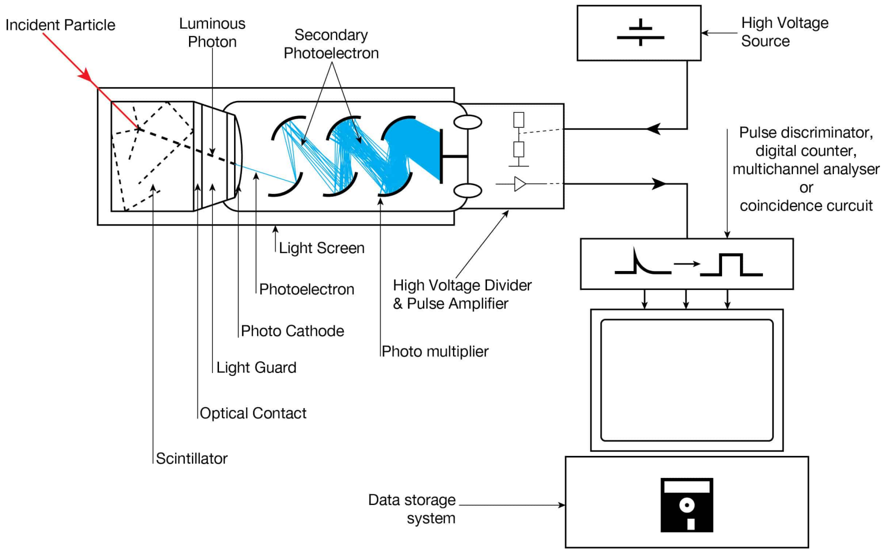

Figure 2: Scintillation Counter with a PMT [2]

- The photons from the scintillator strike the photocathode, releasing primary electrons.
- **Primary electrons** are electrostatically accelerated using a voltage potential. They strike the first dynode and release secondary electrons.
- **Secondary electrons** strike a second dynode, releasing more electrons. This process continues, amplifying the primary signal through 10 to 12 stages of dynodes.
- The **amplified electrical pulse** is produced at the final dynode and connected to the readout system.

3.2.2 Silicon Photo Multipliers (SiPMs)

Instead of a traditional PMT, a SiPM can be used – a pixelated device where each pixel, or microcell, is a series combination of an avalanche photodiode (APD) and a resistor (RQ). All of the microcells are connected in parallel.

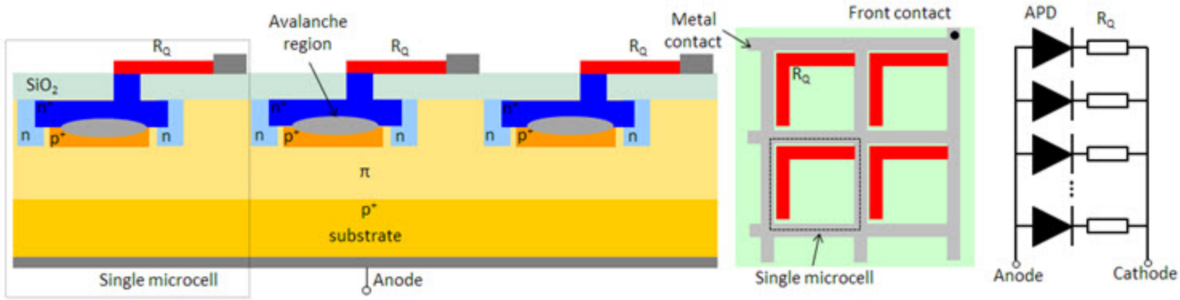

Figure 3: Operation of an SiPM[3]

The first diagram shows the cross-section of the SiPM, and the last shows the corresponding electrical circuit.

- When an SiPM absorbs a photon, the resulting charge carrier, an electron or hole, can trigger an avalanche in the gain region, shown as the grey oval.
- This can create $10^5 - 10^6$ carriers, constituting the gain of the incident carrier.
- The role of the quenching resistor R_Q is to restore the structure into Geiger mode, allowing the photodiode to be ready for another detection.
- The gain causes an amplified current pulse (Figure 4) to flow through the terminals of the SiPM.

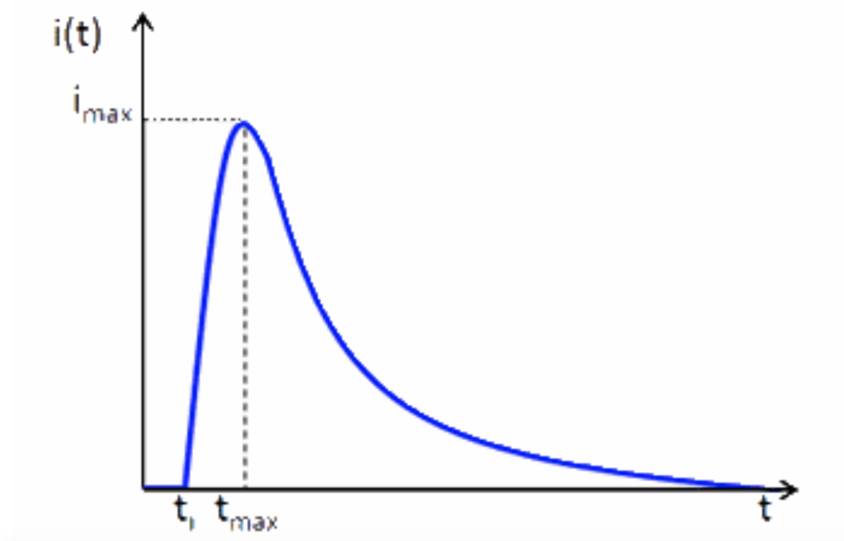

Figure 4: A SiPM Pulse Waveform[3]

4 Experiment Design

4.1 Experimental Setup

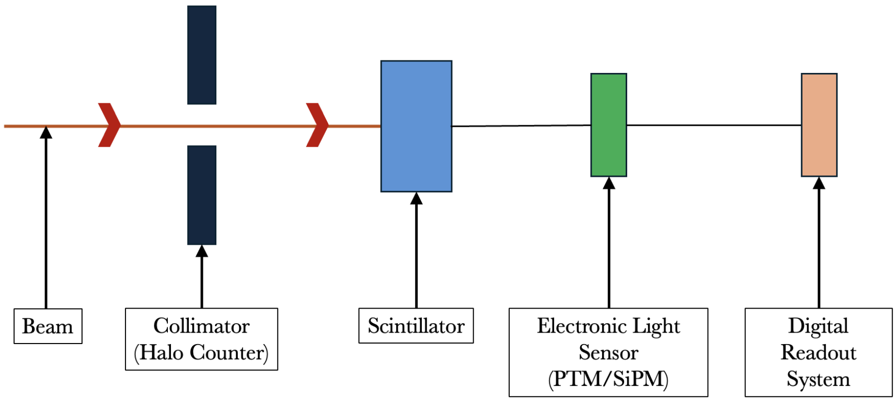

Figure 5: Labelled Diagram of Experimental Setup

At CERN, we'll use the 1-26 GeV T9 beamline; at DESY, we'll use the 1-6 GeV electron beam. Our experimental setup will be the same at both venues. We'll conduct the procedure twice: first with the PMT and then with the SiPM. A collimator will ensure that the effect of the deviated particles is minimised.

4.2 Data Collection Procedure

Our procedure involves increasing the radiation energy of the beam and measuring the response in output voltage.

Since the energy ranges differ at CERN and DESY, we'll use:

- CERN: 1.0 to 15.0 GeV.
- DESY: 1.0 to 6.0 GeV.

The metrics for comparison we'll use are:

- Dynamic Range
- Sensitivity
- Timing Resolution
- Signal-to-Noise Ratio (SNR)

4.2.1 Calibration

We must calibrate both sensor systems to ensure that the output voltage responds linearly to the range of beam energies. This will involve using:

- Mathematical tools like Linear Law
- Pilot Readings

4.2.2 Dynamic Range (DNR)

Dynamic Range measures the spread of the possible output voltages.

1. Record output signals at regular intervals in increments of 0.5 GeV of beam energy.
2. Note the energy at which:
   (a) Linear response begins (lower limit $V_{\min}$)
   (b) Saturation of detector response occurs − graphically, the upper limit of linear response ($V_{\max}$).

The Dynamic Range (in dB) of the electronic light sensor is given as follows:

$$\text{DNR} = 20\log_{10}\left(\frac{V_{\max}}{V_{\min}}\right)\ \text{dB}$$

4.2.3 Sensitivity

Sensitivity measures the extent to which the voltage signal changes with a change in beam energy.

1. Gradually increase radiation energy in increments of 0.5 GeV till V_{max}.
2. Plot the output voltage signal as a function of beam energy.

Since the graph is expected to be linear between $\text{V}_{\min}$ and $\text{V}_{\max}$, the **gradient** of the graph obtained gives the sensitivity of the detector.

4.2.4 Timing Resolution (T_R)

T_R compares the response times of the two detectors. We plan to use:

- A pulsed radiation source capable of firing protons/electrons at regular intervals.
- A high-accuracy timing setup to capture the time between radiation emission and signal detection.

The timing resolution T_R can be calculated as:

$$T_R = T_{\text{Signal Detected}} - T_{\text{Pulse Emitted}}$$

4.2.5 Signal-to-Noise Ratio (SNR)

The signal-to-noise ratio refers to the strength of the desired signal relative to background noise (undesired signal).[4]

1. Record baseline noise level in the absence of any radiation input.
2. Set the beam energy to 10.0 GeV at CERN or 5.0 GeV at DESY.
3. Note the signal's amplitude (A_{Signal}) with this radiation.
4. Calculate the signal-to-noise ratio (in dB) as follows:

$$\text{SNR} = 20 \log_{10} \left(\frac{A_{\text{Signal}}}{A_{\text{Noise}}} \right) \text{ dB}$$

4.2.6 Sample Signal with Noise Events

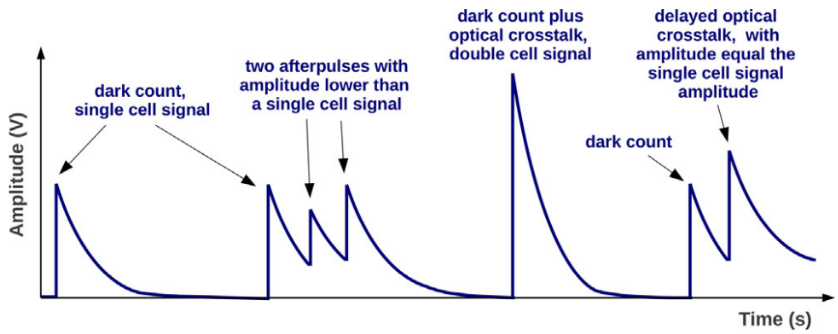

Figure 6: Expected SiPM Output Signal with different kinds of Noise Events[5]

This figure depicts a sample graph of output voltage in response to different types of noise events, which will help us in explaining the noise levels.

4.3 Data Analysis

The desired results for a superior photon detector would be:

1. Higher Dynamic Range (DNR)
2. Higher Sensitivity
3. Lower Timing Resolution
4. Higher Signal-to-Noise Ratio

A standard weightage formula helps account for these factors in selecting the better electronic light sensor:

$$W_1\left(\frac{\text{DNR}_{\text{SiPM}}}{\text{DNR}_{\text{PMT}}}\right)+W_2\left(\frac{\text{Sensitivity}_{\text{SiPM}}}{\text{Sensitivity}_{\text{PMT}}}\right)+W_3\left(\frac{T_{R_{\text{PMT}}}}{T_{R_{\text{SiPM}}}}\right)+W_4\left(\frac{SNR_{\text{SiPM}}}{SNR_{\text{PMT}}}\right)$$

While DNR, Sensitivity, and SNR correlate positively with the detector's quality, a lower timing resolution indicates a better detector. Hence, the ratio has been reversed for T_R.

Typically, sensitivity is the most important factor, followed by DNR, T_R, and lastly SNR. So, we can assign values to the weightages as follows:

- DNR: $W_1 = 0.3$
- Sensitivity: $W_2 = 0.4$
- T_R: $W_3 = 0.2$
- SNR: $W_4 = 0.1$

Thus, our final formula for detector efficiency (DE) ratio becomes:

$$DE = 0.3\left(\frac{\text{DNR}_{\text{SiPM}}}{\text{DNR}_{\text{PMT}}}\right)+0.4\left(\frac{\text{Sensitivity}_{\text{SiPM}}}{\text{Sensitivity}_{\text{PMT}}}\right)+0.2\left(\frac{T_{R_{\text{PMT}}}}{T_{R_{\text{SiPM}}}}\right)+0.1\left(\frac{SNR_{\text{SiPM}}}{\text{SNR}_{\text{PMT}}}\right)$$

$DE > 1$ indicates that SiPM is superior, while $DE < 1$ indicates the opposite. This decision is purely scientific: we must also analyse the equipment's cost as a fifth factor of choice.

Note: These weightages are provisional and might be subject to change if we later find that a certain criterion is more important than we presumed.

5 Limitations

The number of photons emitted by a scintillator is not always directly proportional to the energy of the charged particles that hit them due to a phenomenon called quenching: the annihilation of energy without the emission of a photon.

This is given by Birks's Law: $$\frac{dL}{dx} = S\,\frac{\frac{dE}{dx}}{1 + kB \times \frac{dE}{dx}}$$

- L : Light Yield
- S : Scintillator Efficiency

- kB : Birks's Coefficient
- $\frac{dE}{dx}$: Particle's specific energy loss per unit path length

The experiment also did not consider the effect of **magnetic fields** or the principle of **dark current**.

6 What We Hope to Take Away from the Experience

According to literature, SiPMs are insensitive to magnetic fields, mechanically compact, and require a low voltage to operate. Conversely, the linearity of the pulse height spectrum may vary, while they are also prone to noise at higher temperatures. We hope that our experiment will provide further insight into such experimental findings.

Working on the proposals for BL4S has been an enriching experience for us physics enthusiasts. Through the entire process of submitting a proposal, we've gained exposure to details about particle physics, considerations to be made while proposing an experiment, and the various applications of particle physics research around us. It's been a boost towards our career aspirations in the field of STEM and the chance to perform our experiment will provide a great impetus to our careers.

7 Acknowledgements

We would like to extend our heartfelt gratitude and appreciation to the following people and organisations:

- **Our School, DAIS:** For providing us with the resources required for scientific exploration and increasing our intellectual capabilities.
- **Our School Mentors:** Mr Murali S and Dr. Chandana Ghosh for introducing us to this competition, and graciously guiding us through this process.
- **Our National Contacts:** Dr. Gunn Khatri for clarifying any technical, particle-physics-related doubts we had.
- **CERN BL4S's Team:** For continuously responding to our doubts, requests, and queries on emails (Sarah Maria Zoechling), and for hosting an incredible competition for high school students.

Thank you.

References

[1] BL4S, CERN. 2024. "Beam and Detectors Beamline for Schools 2024." https://beamline-for-schools.web.cern.ch/sites/default/files/Beams_Detectors_BL4S2024.pdf.

[2] "Scintillation Counter - Principle of Operation - Description." n.d. Nuclear Power. https://www.nuclear-power.com/nuclear-engineering/radiation-detection/scintillation-counter-scintillation-detector/scintillation-counter-principle-of-operation/.

[3] "What Is an SiPM and How Does It Work? — Hamamatsu Photonics." n.d. Hub.hamamatsu.com. https://hub.hamamatsu.com/us/en/technical-notes/mppc-sipms/what-is-an-SiPM-and-how-does-it-work.html.

[4] Networking. 'What Is Signal-to-Noise Ratio and How Is It Measured?' https://www.techtarget.com/searchnetworking/definition/signal-to-noise-ratio.

[5] Stefan Gundacker and Arjan Heering 2020 Phys. Med. Biol. 65 17TR01

An Investigation into the Radiation Hardness of Semiconductors for Space Applications

The Quantum Entanglers

Aadi Kothari, Aarav Jalan, Aarav Shah, Annan Vora,
Dhruv Chopra, Keshav Mohta, Kiara Maniar, Param Davda,
Raahil Mullick, Rishi Mody, Ritisha Bansal.

Dhirubhai Ambani International School, Mumbai, India.

April 2024

Contents

1 Introduction and Motivation

BL4S offers a unique opportunity for us to engage in hands-on research in particle physics using cutting-edge technology. Performing this experiment at CERN/DESY would demonstrate our commitment to advancing scientific exploration of the universe. Semiconductors are crucial components in spacecraft electronics, essential for communication, navigation, and data processing. Given that spacecrafts are exposed to high levels of radiation in space conditions, studying the radiation hardness of semiconductors is vital for ensuring the reliability and durability of onboard systems.[1]

2 Aim of the Experiment

The experiment aims to compare the radiation hardness of n-type doped **Silicon Carbide (SiC)** and **Gallium Nitride (GaN)** with a doping concentration of around 10^{14} to 10^{16} dopant atoms per cm^3 for use in spacecraft. To achieve n-type doping, SiC could be doped with nitrogen atoms and GaN with silicon atoms using methods such as ion implantation. Semiconductor samples would be doped and prepared before the experiment at CERN/DESY.

3 Reproduction of Space Conditions

3.1 Types of Particles

Spacecrafts face several different sources of radiation:[2]

1. **Particles Trapped in the Earth's Magnetic Field**: Earth's magnetosphere traps electrons, protons, and sometimes heavy ions. The motion of these charged particles around the Earth forms two primary radiation bands. Most satellites operate in orbits between 1.2 and 10 Earth radii. Figure 1 depicts the distribution of proton flux as a function of earth radii at various energies.

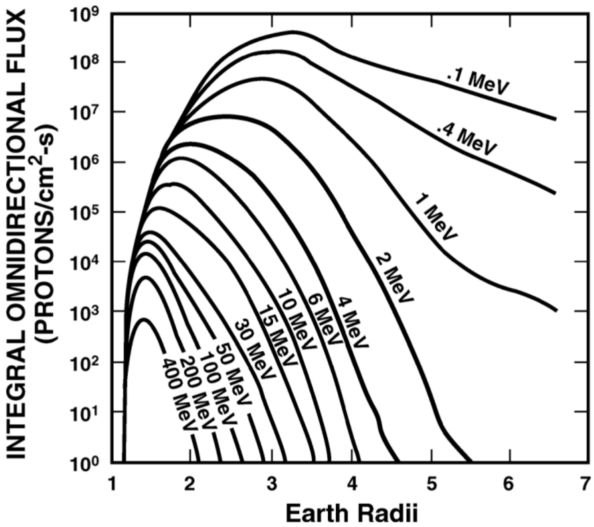

Figure 1: Distribution of Proton Flux as a function of Radial Distance at various energies

Electrons are present up to 12 earth radii in Van Allen radiation belts with energies up to 10 MeV. The particle flux can vary depending upon the axial and equatorial distance from Earth, as depicted in Figure 2.

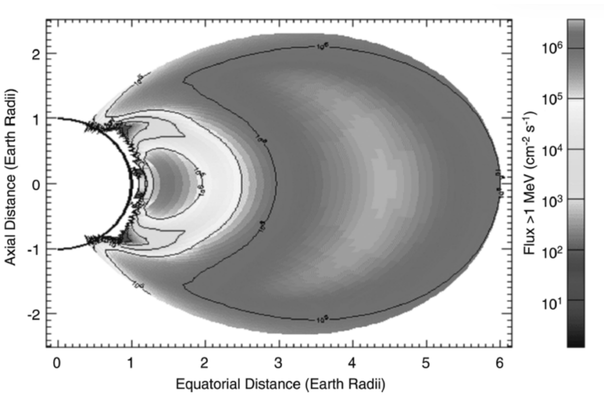

Figure 2: Electron flux

2. **Galactic Cosmic Rays**: Cosmic rays originate from outside the solar system and are omnipresent. They are primarily composed of protons (85%) and alpha particles (14%).

3. **Solar Particle Events**: The composition is the same as in cosmic rays but with $\approx 10^4$ times more protons and alpha particles.

3.2 Theoretical Effects of Radiation

Damage mechanisms include the following:[3]

- **Lattice Displacement**: Primarily caused by neutrons, protons, alpha particles, and heavy ions. They can cause changes in the arrangement of atoms in the crystal lattice of a semiconductor. This can increase the number of recombination centres[1] (causing reduced carrier lifetime, device performance, and efficiency) and reducing the number of minority charge carriers.
- **Ionization Effects**: These are caused by charged particles, even those with low energy. They cause glitches and soft errors.

These mechanisms can cause the following **end results**:

1. High energy protons may each generate thousands of electron/hole pairs in the semiconductor (depending on p-type or n-type doping) by ionization thereby affecting its performance.
2. **Indirect Ionization:** Protons can cause significant upset rates due to indirect mechanisms. Elastic collisions can cause Si/Ge atoms to recoil, alpha/gamma particles to be emitted and spallation reactions[2] to occur. Since emitted particles are much heavier than incoming protons, they deposit higher charge densities as they travel causing single-event effects (including lattice displacement).
3. **Displacement effects**: High-energy protons can collide with atoms in the lattice, causing the atom to recoil. The atom might be knocked free from the lattice leaving a vacancy or displacing other atoms. Such effects reduce the lifetime of charge carriers and can cause carrier removal.

3.3 Experimental Setup

Typical energies of particles described above:

1. Trapped protons in the Earth's magnetosphere have energies up to 500 MeV or 0.5 **GeV**.[4]
2. Electrons in the magnetosphere have maximum energies of $\approx 5-7$ MeV (Figure 2). These energies are too low to be recreated at T9/DESY.
3. Galactic cosmic rays have energies between between 0.1 MeV and 10 GeV with an average of $0.3-0.5$ GeV.[5]
4. Solar cosmic rays usually have particle energy of ≈ 1 GeV. Solar particle events have particle energies of ≈ 2 GeV.[6]

Therefore, the most common particles needed to resemble space conditions are protons. So, the **positive secondary beam at CERN** will be used with protons at 0.5 GeV. The semiconductor sample will be a round crystal cylinder of diameter 2 cm (size of beam's focal point) and length 0.1 cm.

[1]Recombination is the process by which charge carriers (electrons and electron holes) in semiconductors are eliminated. A recombination centre is where this process occurs.

[2]Reactions in which the nucleus (Si/Ge) breaks down into 2 fragments.

4 Quantifying Radiation-Based Damage

4.1 Detectors

The schematic below shows the setup used.

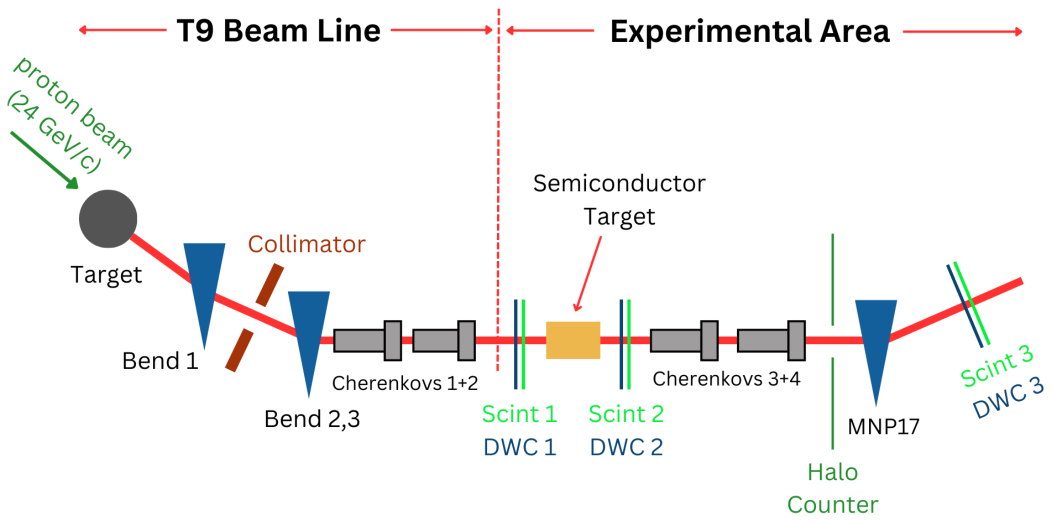

Figure 3: Labelled Diagram of Experimental Setup Made on Canva

1. The initial proton beam from the PS collides with the target, producing various particles.
2. Bending magnets and collimator select the protons moving at 0.5 GeV for the secondary beam.
3. Cherenkov Detectors 1+2, the Scintillator 1 and the DWC 1 allow accurate detection of whether a particle passed by and the type of the particle.
4. After the semiconductor, a second scintillator, DWC detector, and set of Cherenkov detectors is placed (Scint2, DWC2, Cherenkovs 3 and 4). These detect any particles that pass through the semiconductor material and whether they are protons, in which case the lattice structure of the semiconductor has been disturbed.
5. The magnetic spectrometer, consisting of the MNP17 dipole magnet, DWC 3, and scintillator SCINT 3, helps detect the change of momentum of protons after interacting with the semiconductor and any lattice damage.

4.2 Detection of Other Characteristics

The electrical properties of the semiconductor can be compared by performing the tests given below **before and after irradiation.**

Electrical measurement instruments needed include:

- Voltage Source
- Ammeter
- Voltmeter
- Oscilloscope
- Multi-meter

Measured characteristics include:

1. **Current-Voltage (I-V) Characteristics:** Measure the current flowing through the semiconductor as a function of applied voltage, using a voltage source and ammeter. This provides information on:
   - Threshold Voltage: The minimum voltage required for current to flow. A shift in this voltage implies changes in the semiconductor's conductivity and carrier transport properties.
   - Leakage current: The current that flows when the ideal current is supposed to be 0. An increase in the leakage current in the I-V curve signifies enhanced carrier trapping and recombination.
2. **Resistance:** Apply a constant voltage and measure the resistance using the multi-meter, at a constant temperature. These measurements provide information on defects such as lattice vacancies, particle dislocations, and impurities in the semiconductor lattice, which lead to increased resistivity. Increased resistivity reflects reduced carrier mobility and higher radiation damage.
3. **Capacitance Voltage Characteristics**: Represents the variation of capacitance with voltage and changes in doping profile. The C-V curve features accumulation, depletion, and inversion regions, corresponding to different charge distributions. Shifts or broadening of peaks in the curve correspond to variations in carrier density. Radiation damage can modify the doping profile by creating lattice defects. Displacement damage disrupts the crystalline structure, leading to changes in the distribution of **dopant atoms** within the lattice, affecting electrical conductivity and carrier mobility.

4.3 Transient Current Technique

Transient Current Technique (TCT)[7] is based on the measurement of the induced current transient of drifting charge carriers in the semiconductor under the influence of an electric field E. The $e/h-$ pairs will be created by the illumination of a reversely biased sensor with 70 ps laser light pulses causing the charge carriers to drift towards their respective electrode and induce a current signal that can be measured as a function of time. **Ramo's Theorem** states that the induced current signal $I_{e,h}(t)$ can be expressed as:

$$I_{e,h}(t) = \frac{q_0 N_{e,h}(t)}{d} v_{\mathrm{drift}_{e,h}}(t) \tag{1}$$

for a fully depleted sensor.

- $N_{e,h}$: Number of charge carriers
- $v_{\text{drift}_{e,h}}$: Drift Velocity

The drift velocity is dependent on E and the mobility of charge carriers $\mu_{e,h}$ as:

$$v_{drift_{e,h}} = \mu_{e,h}(E)E \tag{2}$$

Depending on the creation region of charge carriers, TCT may obtain parameters like electron and hole signature lifetimes (τ) and Charge Collection Efficiency (CCE), where:

$$CCE = \frac{Q}{Q_0} \tag{3}$$

- Q : Collected charge
- Q_0 : Injected charge

when the deposited number of charge carriers $Q_0 = q_O N_0$. The collected charge can be calculated using:

$$Q = \int I_e(t)dt + \int I_h(t)dt \tag{4}$$

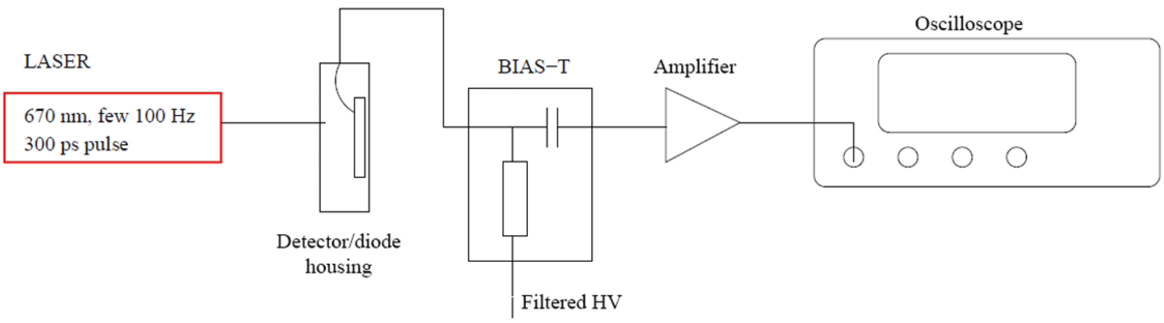

Figure 4: Transient Current Setup [8]

The laser pulses generate charge carriers at the detector surface which travel under the surface of the electric field inside the detector and induce current in the readout electrodes. This current signal is amplified and shown on the oscilloscope.

4.4 Deep Level Transient Spectroscopy (DLTS)

This method requires additional apparatus. Check the **Appendix** for more details.

5 What We Hope to Take Away from the Experience

Working on the BL4S competition has been an enriching experience for us, and we have learned a lot about Particle Physics through the course of our research. It's been a boost towards our career aspirations in the field of STEM, and we hope to share this knowledge with those in our community as well.

6 Acknowledgements

We would like to extend our heartfelt gratitude and appreciation to the following people and organisations:

- **Our School, DAIS:** For providing us with the resources required for scientific exploration and increasing our intellectual capabilities.
- **Our School Mentors:** Mr. Murali S and Dr. Chandana Ghosh for introducing us to this competition, and graciously guiding us through this process.
- **Our National Contacts:** Dr. Gunn Khatri for clarifying any technical, particle-physics-related doubts we had.
- **CERN BL4S's Team:** For continuously responding to our doubts, requests, and queries on emails (Sarah Maria Zoechling), and for hosting an incredible competition for high school students.

Thank you.

References

[1] Team, Tessolve. "Chandrayaan 3: How Semiconductors Are Powering India's Space Ambitions." Tessolve (blog), December 12, 2023. https://www.tessolve.com/chandrayaan-3-how-semiconductors-are-powering-indias-space-ambitions/.

[2] J. R. Schwank, M. R. Shaneyfelt and P. E. Dodd, "Radiation Hardness Assurance Testing of Microelectronic Devices and Integrated Circuits: Radiation Environments, Physical Mechanisms, and Foundations for Hardness Assurance," in IEEE Transactions on Nuclear Science, vol. 60, no. 3, pp. 2074-2100, June 2013, doi: 10.1109/TNS.2013.2254722.

[3] Belousov, Anton, Moskau, and Russland. 2014. "Radiation Effects on Semiconductor Devices in High Energy Heavy Ion Accelerators -Darmstadt -D17." https://d-nb.info/1110979703/34#: :text=Radiation%20effects%20on%20silicon%20components.

[4] E. G. Stassinopoulos and J. P. Raymond, "The space radiation environment for electronics," Proc. IEEE, vol. 76, no. 11, pp. 1423–1442, Nov. 1988.

[5] "Cosmic Rays - Richard Mewaldt." Accessed April 10, 2024. https://sites.srl.caltech.edu/ rmewaldt/cos_encyc.html#: :text=Most%20galactic%20cosmic%20rays%20have,of%2010%20increase %20in%20energy.

[6] "Pierre Auger Observatory," October 12, 2012. https://web.archive.org/web/20121012090629/ http://www.auger.org/cosmic_rays/faq.html#how_many.

[7] Hamburg, Coralie, Fachbereich Physik, Erika Garutti, and Wolfgang Hansen. 2013. "Impact of Irradiations by Protons with Different Energies on Silicon Sensors." https://cds.cern.ch/record/2636089/files/desy-thesis-13-021.pdf.

[8] "TCT -Transient Current Technique." n.d. Accessed April 10, 2024. https://www.tifr.res.in/ icfa2023/assets/doc/TCT_Instructions_ForTheExcercise.pdf.

7 Appendix

7.1 Deep Level Transient Spectroscopy

If **Deep Level Transient Spectroscopy** (DLTS) is available at CERN/DESY, we would use it to investigate electrically active defects by recording capacitance transients as a function of the temperature of the diode to extract the defect concentration N_t, the activation energy δE_a and the capture cross section σ_t.

7.1.1 The DLTS Principle of Detection

1. **Detection of Electron Traps:** A reverse bias creates a depleted region. When decreasing the bias voltage, the depleted region shrinks and electrons flow into the space region containing the majority of carriers and the defects a level below the Fermi level are filled by electrons. On increasing the reverse bias again, the capacitance decreases and the captured electrons are emitted to the conduction band. This capacitance transient has negative polarity causing $C_{\text{final}} < C_R$.

2. **Detection of Hole Traps:** Under a reverse bias, these traps will capture electrons before catching holes. A forward bias is then applied to fill the bulk with majority and minority carriers. On reapplying the reverse bias, the change in capacitance due to the capture of holes by the traps can be measured. The capacitance transient for a hole trap has positive polarity resulting in $C_{\text{final}} > C_R$.

7.1.2 Determination of Defect Parameters

According to the Shockley-Read-Hall statistics, the capture and emission of charge carriers of a defect level can be described as a statistical process. The emission time constant (τ) is the rate at which charge carriers are emitted from a defect and it is dependent on the defect's capture cross-section (σ), the thermal velocity of the charge carriers (v_{th}), the effective density of states in the valence band ($N_{C,V}$) and the activation energy (ΔE_a). Hence:

$$\tau_i = \left[\sigma_i v_{th,i} N_{C,V} \cdot \left(\exp \frac{-\Delta E_a}{k_B T}\right)\right]^{-1}, \ \ i = e, h \tag{5}$$

The activation energy (ΔE_a) is the energy barrier for the charge carriers to be emitted from the defect. It can be determined with the help of an Arrhenius plot:

$$\ln\left(\tau_i v_{th,i} N_{CV}\right) = -(\ln \tau_i) + \frac{\Delta E_a}{K_B T} \tag{6}$$

Thus, the activation energy can be extracted by the slope of the $\ln\left(\tau_i v_{th,i} N_{CV}\right)$ verses $\frac{1}{T}$ and the capture cross-section from the intersection of the ordinate.

The defect concentration N_t is related to the amplitude of the capacitance transient ΔC_0 and the initial defect concentration $N_{eff,0}$ by the equation:

$$N_t \approx 2N_{eff,0}\frac{\Delta C_0}{C_R} \tag{7}$$

The measured capacitance follows an exponential behaviour defined by:

$$C(t) = \Delta C_0 \cdot \exp\left(-\frac{t+t_0}{\tau_i}\right) + C_R \tag{8}$$

Where t_0 denotes delay to avoid pulse overload recovery of the measurement bridge.

The most important measurement method is the temperature scan Tempscan. With variations in the temperature, the band gap is scanned from mid-gap levels to band gap levels. The capacitance transients will then be processed using the correlation function b1-correlator which is the folding of the transient function with a sine function. We will be using three different values for the time window (T_w) which are 10 ms, 500 ms, and 2 s which will allow us to record the emission rates over a large range of temperatures.